Liquid Crystals
Publication details, including instructions for authors and subscription information:
http://www.informaworld.com/smpp/title~content=t713926090

AC electric field induced helix unwinding in planar texture of a ferroelectric liquid crystal

Z. H. Wang[a]; Z. M. Sun[a]; D. Feng[a]
[a] Laboratory of Solid State Microstructures, Nanjing University, Nanjing, P.R. of China

To cite this Article Wang, Z. H. , Sun, Z. M. and Feng, D.(1991) 'AC electric field induced helix unwinding in planar texture of a ferroelectric liquid crystal', Liquid Crystals, 9: 6, 863 — 871
To link to this Article: DOI: 10.1080/02678299108055008
URL: http://dx.doi.org/10.1080/02678299108055008

AC electric field induced helix unwinding in planar texture of a ferroelectric liquid crystal

by Z. H. WANG, Z. M. SUN* and D. FENG
Laboratory of Solid State Microstructures, Nanjing University, Nanjing, 21008, P.R. of China

(*Received 17 September 1990; accepted 21 December 1990*)

The helix unwinding induced by an AC electric field in a thick ferroelectric S_C^* sample with planar orientation has been investigated experimentally. Four patterns of instabilities have been observed below the unwinding critical field E_C. The corresponding thresholds and E_C are found to be dependent on frequency. The formation of two instabilities (λ pattern and rhombic lattice pattern) is discussed on the basis of the present theory. The behaviour above the critical field is briefly described.

1. Introduction

In the S_C^* phase chiral rod-like molecules are tilted in parallel layers. Because of the chirality, the directions in these smectic layers are twisted relative to each other, which results in a helical structure [1]. When an electric field E is applied to a slab of the S_C^* liquid crystal and over a critical value E_C, the helix will be unwound. So far much work has been done using DC electric fields [2–4]. As far as AC electric unwinding is concerned, it is still an unsolved problem, although some efforts have been made by various researchers [5–7]. Recent experiments show that below E_C instabilities may occur at certain frequencies [8, 9]. Therefore, when we study the AC electric unwinding, we should not only consider the coupling between the permanent dipoles and the field, but also must take dielectric and conductive anisotropy as well as electrohydrodynamical effects into account, which further adds to the complexity of the problem. In this paper we report the experimental investigation on the unwinding process of a planar oriented ferroelectric S_C^* liquid crystal under AC electric fields over 0–120 kHz. The experiment reveals the existence of four instabilities below the critical field, and shows the frequency dependence of thresholds and the critical field E_C. These results are discussed on the basis of the current theory. Additionally, some special effects above E_C are briefly described.

2. Experimental

The material used is the chiral ferrolectric FCS 101 mixture. The mesophase transitions are as follows:

$$\mathrm{C}\overset{<0^\circ\mathrm{C}}{\text{———}}\mathrm{S_I}\overset{15\cdot5^\circ\mathrm{C}}{\text{———}}\mathrm{S_C^*}\overset{55\cdot4^\circ\mathrm{C}}{\text{———}}\mathrm{S_A}\overset{76\cdot1^\circ\mathrm{C}}{\text{———}}\mathrm{N^*}\overset{78\cdot7^\circ\mathrm{C}}{\text{———}}\mathrm{I}$$

The sample is sandwiched between two glass plates coated with transparent SnO_2 electrodes. The thickeness of the cell is 25 μm, determined by mylar spacer. An AC

* Author for correspondence.

generator (0–200 Hz) is connected to the electrodes in order to apply an AC sinusoidal electric field across the sample. The glass plates are treated with polyvinyl alcohol and then rubbed unidirectionally to induce a planar alignment. The sample cell is placed in a hot stage fabricated by us and observed under a Leitz polarizing microscope (ORTHOPLAN-POL). The temperature is controlled automatically with the accuracy better than 0·1°C. Homogeneous alignment can be obtained by cooling the sample slowly (1°C/h) from the isotropic liquid to the S_A phase under an AC electric field of 10^3 V/m at $f=20$ Hz. Further cooling without the action of the field results in a well aligned planar texture of the S_C^* phase, as shown in figure 1. A large perfect monodomain with a size of $2\times 1\ \mathrm{mm}^2$ is chosen for observation. All measurements are carried out at $T-T_C=-0{\cdot}5$°C ($T_C=55{\cdot}4$°C).

3. Results and discussion

The texture changes in AC electric unwinding are very complicated. The AC electric field can induce the complex patterns of instabilities below the critical field. Raina once reported a λ-pattern in both DOBAMBC and DOBAMBCC ($f=500$ Hz) [8], while Jakli *et al.* observed sinusoidal undulation and a zig-zag structure in the mixture FK4 ($f=10$ Hz) [9]. In our experiment all three patterns can be observed in FCS 101. In addition, we also find a new rhombic lattice pattern. These patterns appear in certain frequency ranges, similar to instabilities in nematics and cholesterics [10, 11]. Therefore the helix unwinding exhibits different characteristics with frequency. In AC electric unwinding the definition of the critical field is not as easy as that in DC electric unwinding on account of the existence of instabilities. Later we shall point out that the critical field E_C corresponds to the disappearance of the periodic structures relative to the helix (not merely the pitch stripes) and above E_C the flow induces viscous shear torques which unwind the helical texture. The influence of AC electric fields with different frequencies on the helical structure is shown in figure 2, for a FCS 101 sample at $T-T_C=-0{\cdot}5$°C. For the sake of convenience we divide the frequency range 0–120 kHz into seven frequency zones in light of the characteristics of helix unwinding. The frequency range of each zone is marked in figure 2.

In the low frequency region (zone 1, $f=0$–17 Hz) and the high frequency region (zone 7, $f=1{\cdot}5$–120 kHz), the texture changes are comparatively simple. No instabilities appear in the sample. The helical pitch increases under increasing field. Above a

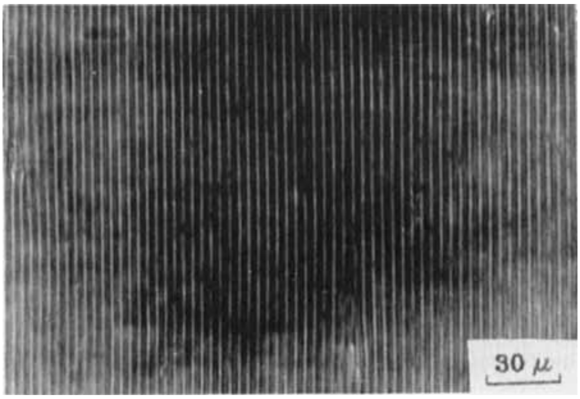

Figure 1. Homogeneous alignment of pitch stripes in the S_C^* phase.

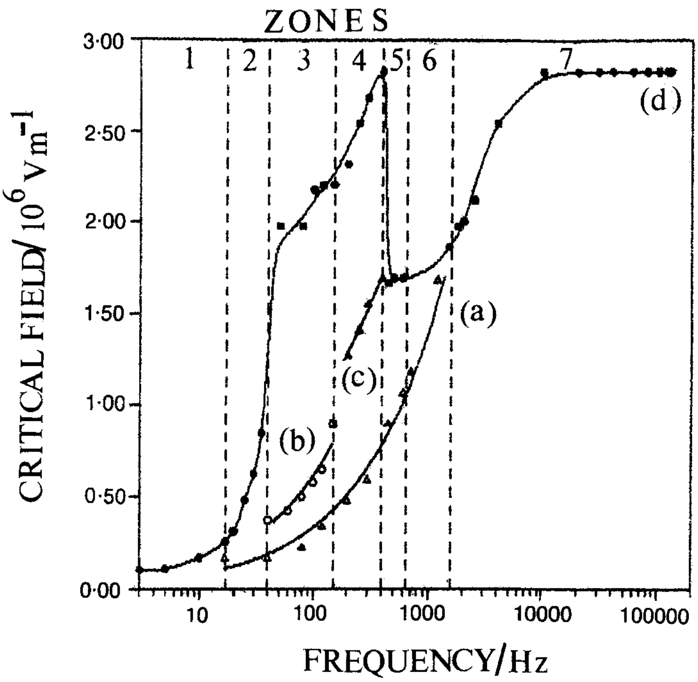

Figure 2. Frequency dependence of various thresholds and the unwinding critical field under the action of AC electric fields.

threshold E_C, the parallel pitch stripes disappear (see zone 1) or are replaced by a flow pattern (see zone 7). In the region of $f = 17$–1500 Hz (see zone 2 to zone 6), at a certain threshold, E_W, an undulation instability occurs. The straight pitch stripes become sinusoidally distorted, as shown in figure 3. E_W is defined as a wavy threshold. The curve (*a*) in figure 2 represents the frequency dependence of E_W. When $E > E_W$, the following texture changes will take place:

(i) In zone 2 ($f = 17$–40 Hz), the wavy stripes disappear gradually when the field E approaches E_C. Hence in zone 1 and zone 2 the texture change is analagous to that under DC field.

(ii) In zone 3 ($f = 40$–150 Hz) and zone 4 ($f = 150$–400 Hz), the pure sinusoidal pattern varies and forms a zig-zag structure (see figure 4). With increase of the field, such a zig-zag pattern can evolve into a rhombic lattice pattern (see zone 3 and figure 5) or a λ pattern (zone 4, see figure 6). The corresponding thresholds are called lattice thresholds E_L and λ threshold E_λ respectively. The curves (*b*) and (*c*) in figure 2 show the frequency dependence of E_L and E_λ respectively. These patterns do not disappear until E increases up to E_C.

(iii) In zone 5 ($f = 400$–650 Hz) and zone 6 ($f = 650$–1500 Hz), the wavy stripes do not evolve into any other regular patterns. At E_C, the periodic structure becomes irregular and the helix is completely destroyed.

The curve (*d*) in figure 2 represents the frequency dependence of the threshold E_C, at which the periodic textures disappear entirely. Here the periodic textures which we refer to are the stripes (zones 1, 2, 5, 6 and 7, straight or wavy) or the rhombic lattice pattern (see zone 3) or the λ pattern (seen zone 4). Since all periodic textures

Figure 3. Sinusoidal undulation instability with a wavelength $L = 100\,\mu$m; $E = 1{\cdot}6 \times 10^5$ V/m; $f = 30$ Hz.

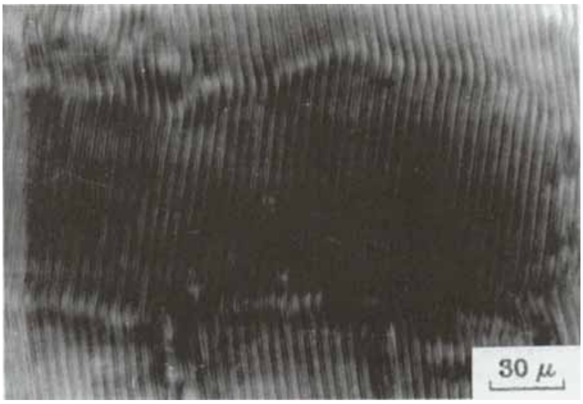

Figure 4. Zig-zag structure. $E = 6{\cdot}8 \times 10^5$ V/m; $f = 150$ Hz.

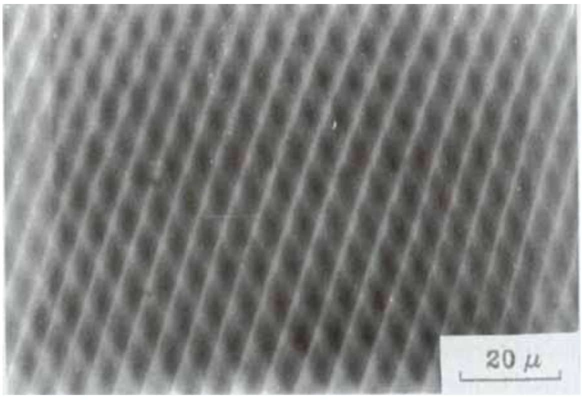

Figure 5. The rhombic lattice pattern. $E = 4{\cdot}3 \times 10^5$ V/m; $f = 50$ Hz.

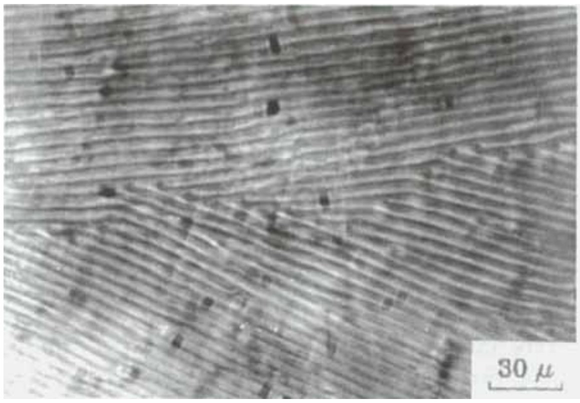

Figure 6. λ pattern. $E=2{\cdot}1\times10^6$ V/m; $f=190$ Hz.

characterize the helical structure, their disappearance means the helix has been unwound. Therefore E_C is actually the unwinding critical field. We notice that in figure 2 the curves (*a*), (*b*) and (*c*) rise monotonically with increase of frequency, which indicates that the distortion of the helix becomes more and more difficult with the increase of frequency. On the other hand, the variation of E_C as a function of frequency is more complex. E_C does not change obviously between 0–17 Hz (see zone 1). This fact shows that the permanent polarization can follow the low frequency field. So we have a ferroelectric regime in zone 1. Beyond these frequencies, E_C increases sharply with frequency, especially for 17–50 Hz. E_C tends to saturate at high frequencies ($f=10$–120 kHz). Evidently, in this frequency range the molecules cannot follow the field and the unwinding is only due to the induced polarization. So we have a dielectric regime and E_C is found to be one order of magnitude higher than E_C in zone 1. These facts coincide with the result reported by Raina [8] and supports the calculated frequency dependence of the unwinding critical field E_C obtained by Jakli *et al.* [12]. In the range of $f=50$–10000 Hz curve (*d*) has a minimum at $f=400$ Hz. This is again in agreement with Raina's experiment for DOBAMBCC [8]. Since both FCS 101 and DOBAMBCC have negative dielectric anisotropy and low permanent polarization, the similarity between the experimental results obtained for both materials is reasonable. Jakli *et al.* also found such a minimum at $f=300$ Hz in a FK4 sample with thickness of 60 μm [9]. Experimentally they observed in the vicinity of this frequency the unwinding is caused by a flow and interpreted this phenomenon theoretically using a simplified model [12]. In our experiment we have not found such a flow with a spatial periodicity equal to that of the zig-zag structure. At $f\leqslant400$ Hz the zig-zag texture evolves into the λ pattern whose structure is stable and difficult to unwind (i.e. E_C is high). At $f\geqslant400$ Hz, no regular patterns occur, and at the lower field the wavy stripes directly split into a great number of random broken bits which oscillate intensely. Therefore the minimum of curve (*d*) in figure 2 is probably related to a more complicated mechanism and does not seem merely attributable to the conductivity of the substance. Further theoretical work is indeed desirable. It must be pointed out that the frequency dependence of thresholds and the critical field shown in figure 2 are related to the temperature. When the temperature changes, the experimental data will change too.

The formation mechanism of the sinusoidal undulation and the zig-zag structure has been explained in [12]. Under increasing field, the zig-zag texture can evolves into either a rhombic lattice pattern or a λ pattern in FCS 101. That means two changes may take place in the evolution of the zig-zag structure. Now let us make a qualitative discussion of it on the basis of the theoretical frame presented before [12]. Here an experimental fact has to be mentioned, that is, our experimental observation supports the model of an antiparallel spontaneous polarization boundary condition put forward by Glogarova *et al.* [13]. Under the polarizing microscope we observe two dechiralization line arrays which are situated near both upper and lower surfaces and are shifted by half pitch.

When an AC electric field is applied to a planar sample, there is a component of the field, E_z, along the helical axis owing to the conductivity anisotropy and the dielectric anisotropy. E_z will induce the sinusoidal undulation of smectic layers as well as a zig-zag structure [12]. Experimentally we find at higher fields the amplitude of zig-zag can still increase. But such distortion has a limitation. Therefore, when the field is even higher, we observe the following two phenomena:

(i) If the angle ψ of kink in the zig-zag structure is not large enough, under the action of the field, the kinks in upper and lower arrays will move along two different directions, as shown in figure 7 (*a*). Consequently, the zig-zag texture evolves into two twisted line arrays shown in figure 5. We suppose that at high field the zig-zag dechiralization lines are not stable as a result of too high distortion free energy, and under the action of the line tension they will be straightened through the motion of kinks so as to reduce the distortion free energy. Hence the rhombic lattice pattern is in fact two parallel line arrays twisted relative to each other. This has been confirmed experimentally. Under the polarizing microscope, we find that these two parallel line arrays are indeed not in the same plane when we focus the objective on different planes.

(ii) If the angle ψ of kink is large enough, we observe that the kinks in upper and lower line arrays move along the same direction and annihilate, as shown in figure 7 (*b*). Because of motion and annihilation of kinks, the sample consists of a number of small monodomains with different orientations (note these orientations deviate the original orientation). On the boundary of small monodomains we can see the λ pattern (see figure 6). So the λ pattern is similar to a type of grain boundary defect in crystals. According to this experimental fact we suppose that if the angle of kink is large enough, it can reduce the distortion free energy more effectively to form a λ pattern than a rhombic lattice pattern. In fact, as shown in figures 5 and 6, the obtuse angle of λ patterns is 154°, indeed larger that that of the rhombic lattice pattern (130°). Besides, we find the angle of the rhombic lattice increases with frequency. When the angle is large enough, the rhombic lattice pattern cannot exist, instead the λ pattern emerges. This fact means the frequency region of the λ pattern is higher than that of the rhombic lattice pattern, as shown in figure 2.

Except for the instabilities, we have yet found very spectacular effects when the field is above E_C. In zone 2, the wavy stripes disappear at $E = E_C$. But at $E > E_C$, we can see an incomplete lattice pattern emerge, as shown in figure 8. A square lattice pattern can also be observed in zone 6 at $E > E_C$ (see figure 9). These lattice patterns are different from the rhombic lattice pattern which emerges below E_C in zone 3. They appear at $E > E_C$, and when the field decreases down to $E < E_C$, they disappear and the pitch stripes reappear. At even higher fields these lattice patterns are replaced by a flow. Similar regular patterns above the thresholds have been observed in cholesterics [11]. However, such effects are reported for the first time in the S_C^* phase. Finally, we should

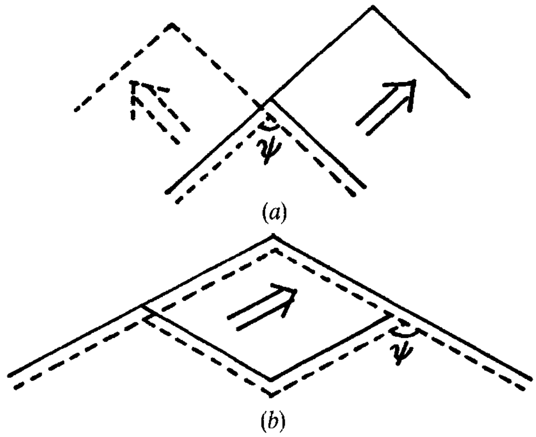

Figure 7. Evolution of the zig-zag structure (*a*) The kinks in upper and lower line arrays move along two directions respectively. (*b*) The kinks in upper and lower line arrays move along the same direction and annihilate.

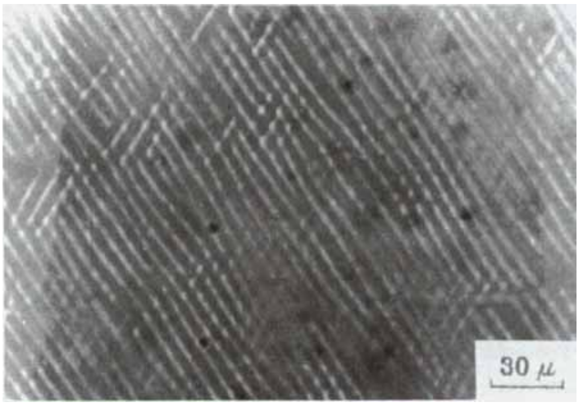

Figure 8. Incomplete lattice pattern above E_C in zone 2. $E = 1{\cdot}5 \times 10^6$ V/m; $f = 30$ Hz.

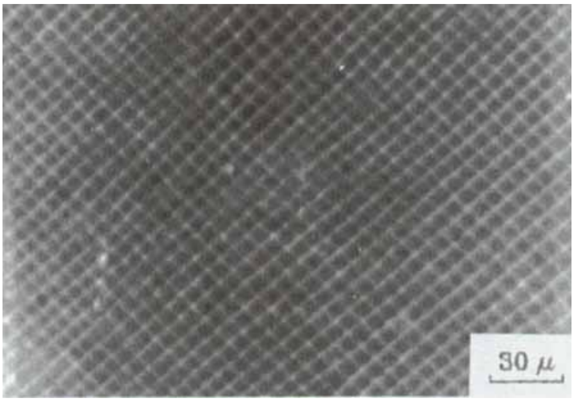

Figure 9. Square lattice pattern above E_C in zone 6. $E = 2{\cdot}0 \times 10^6$ V/m; $f = 800$ Hz.

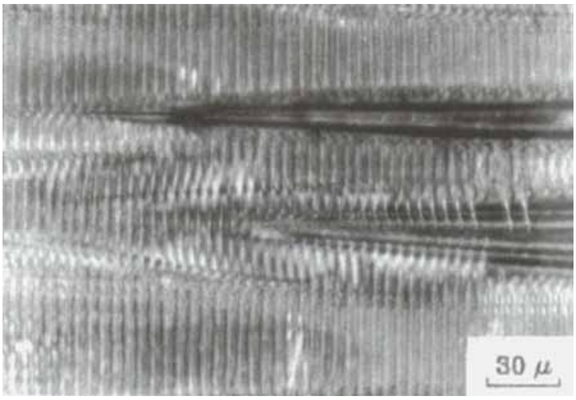

Figure 10. Edge-like flow pattern appears along the direction perpendicular to the parallel pitch stripes from the boundary of monodomains below E_C. $E=2{\cdot}2\times10^6$ V/m; $f=100$ kHz.

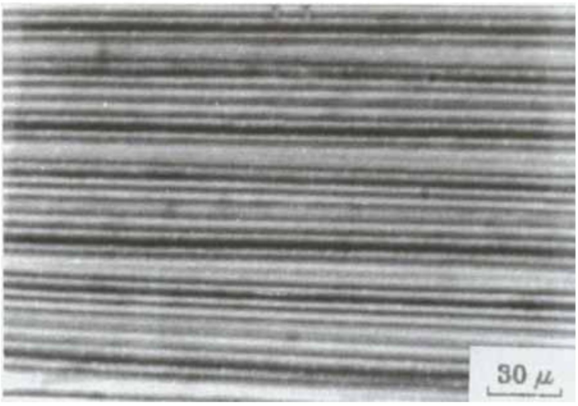

Figure 11. Flow pattern at $E_C=2{\cdot}8\times10^6$ V/m; $f=100$ kHz.

point out that the fluid flow is not always the same for all frequencies. In the low frequency region ($f<1500$ Hz), the fluid flow shows colour and turbulence. In the high frequency region (see zone 7), when the field E approaches E_C, an edge-like pattern appears along the direction perpendicular to the parallel stripes at a constant speed from the boundary of monodomains (see figure 10). At $E=E_C$, all pitch stripes disappear and we are only left with this regular pattern of the fluid flow (see figure 11). However, in the focal conic texture, such edge-like patterns cannot be observed.

The effects cited above should be investigated by further work. They present an important and interesting subject for investigation on electrohydrodynamics in the S_C^* phase. We believe that in order to solve these problems it will be helpful to understand AC electric unwinding.

4. Conclusion

In this paper the helix unwinding of a planar oriented S_C^* phase under AC electric field has been investigated over a wide frequency range. We have observed four patterns of instabilities below the critical field in a FCS 101 sample, a λ pattern and a rhombic pattern can be thought of developing from the zig-zag structure. Because of negative dielectric anisotropy and low polarization the frequency dependence of the critical field E_C for this mixture in the S_C^* phase is similar to that for DOBAMBCC [8]. Above E_C two regular patterns can also be observed at certain frequencies. These experimental results have to be interpreted using a more satisfactory theory.

The authors are grateful to Dr. Schadt at the F. Hoffmann-La Roche Company, Switzerland, for kindly supplying the FCS 101 mixture. This work was supported by the National Natural Science Foundation of China under the grant No. 1870714.

References

[1] MEYER, R. B., LIEBERT, L., STREZELECKI, L., and KELLER, P. J., 1975, *J. Phys. Lett., Paris*, **36,** L69.
[2] HANDSCHY, M. A., and CLARK, N. A., 1983, *Phys. Rev. Lett.*, **51,** 471.
[3] PH. MARTINOT-LAGARDE, DUKE, R., and DURAND, G., 1981, *Molec. Crystals liq. Crystals*, **75,** 249.
[4] GLOGAROVA, M., LEJCEK, L., PAVEL, J., JANOVEC, V., and FOUSEK, J., 1983, *Molec. Crystals liq. Crystals*, **91,** 309.
[5] PARMAR, D. S., RAINA, K. K., and SHANKAR, J., 1983, *Molec. Crystals liq. Crystals*, **103,** 77.
[6] LABROO, B., RAZDAN, V., PARMAR, D. S., and DURAND, G., 1985, *J. Phys. Lett., Paris*, **46,** L-1177.
[7] ROUT, D. K., and CHOUDHARY, R. N. P., 1988, *Ferroelectrics*, **82,** 157.
[8] RAINA, K. K., 1987, *Molec. Crystals liq. Crystals*, **151,** 211.
[9] JAKLI, A., BATA, L., and EBER, N., 1988, *Ferroelectrics*, **85,** 187.
[10] DUBOIS-VIOLETTE, E., DURAND, G., GUYON, E., MANNEVILLE, P., and PIERANSKI, P., 1978, *Liquid Crystals*, edited by L. Liebert (Academic Press), p. 147.
[11] AROULD-NETILLARD, H., and RONDELEZ, F., 1974, *Molec. Crystals liq. Crystals*, **26,** 11.
[12] JAKLI, A., JANOSSY, I., and BATA, L., 1988, *Ferroelectrics*, **88,** 73.
[13] GLOGAROVA, M., FOUSEK, J., LEJCEK, L., and PAVEL, J., 1984, *Ferroelectrics*, **58,** 161.